

Temperature-dependent Drude transport in a two-dimensional electron gas

D. S. Novikov

Department of Physics, Yale University, New Haven, Connecticut 06520

(Dated: February 14, 2009)

We consider transport of dilute two-dimensional electrons, with temperature between Fermi and Debye temperatures. In this regime, electrons form a non-degenerate plasma with mobility limited by potential disorder. Different kinds of impurities contribute unique signatures to the resulting temperature-dependent Drude conductivity, via energy-dependent scattering. This opens up a way to characterize sample disorder composition. In particular, neutral impurities cause a slow decrease of conductivity with temperature, whereas charged impurities result in conductivity growing as a square root of temperature. This observation serves as a precaution for literally interpreting metallic or insulating conductivity dependence, as both can be found in a classical metallic system.

PACS numbers: 72.10.-d 73.40.-c 71.30.+h 81.05.Uw

I. INTRODUCTION

Electron transport is conventionally understood within the Fermi liquid theory framework.¹ In a Fermi liquid (FL), screening of the offset charge is very efficient due to large density of states. As a result, effective disorder potential for quasiparticles is always short-ranged. The latter leads to temperature-independent Drude conductivity, while interaction effects provide corrections to the Drude transport in the powers of small parameter T/ϵ_F , where T is temperature ($k_B = 1$), and ϵ_F is the Fermi energy. These corrections originate due to scattering off the Friedel oscillations,^{1,2} and due to temperature dependence of the random-phase approximation (RPA) screening.³

What happens when the carrier density n is reduced so much that the system becomes non-degenerate, $T > \epsilon_F$? In this case the Fermi energy is irrelevant, and the system is essentially a classical plasma (Fig. 1). Such a situation may occur in actively studied clean dilute heterostructures^{4,5,6,7,8,9,10} where $n \lesssim 10^{10} \text{ cm}^{-2}$, with record densities down to $7 \times 10^8 \text{ cm}^{-2}$ (Ref. 8). These densities correspond to $\epsilon_F \sim 10 - 100 \mu\text{V} \sim 0.1 - 1 \text{ K}$. Transport in such a system will depend on the strength e^2/a of electron interactions relative to temperature (here $a = 1/\sqrt{\pi n}$ is the Wigner-Seitz radius, and the dielectric constant κ is included into the definition of charge, $e^2 \rightarrow e^2/\kappa$, for brevity). For strong interactions, $e^2/a > T$, we have a strongly-correlated semiclassical electron “liquid” whose collective modes are likely to affect transport.^{11,12}

Here we consider the two-dimensional (2D) transport in the opposite, weakly-interacting regime,

$$\epsilon_F, e^2/a \ll T \ll \Theta_D. \quad (1)$$

We assume that temperature is high enough so that carriers form a classical weakly-interacting plasma, yet is well below the Debye temperature Θ_D so that the phonon contribution to transport can be either neglected or subtracted in a controlled way. Transport is then dominated by the practically *unscreened* potential disorder. Such a situation can become relevant in the cleanest heterostructures (e.g. Ref. 8), where, for the lowest densities, the

interaction energy $e^2/a \approx 5 \text{ K}$ is one order of magnitude below the Debye temperature. With increasing sample quality, the carrier density decreases and the applicability range (1) widens. Another system where the present approach may be applicable is graphene with the substrate-induced gap, as described towards the end of the paper.

We show that in the regime (1), the Drude conductivity $\sigma(T)$ becomes strongly temperature-dependent. Its temperature dependence originates from the energy-dependent impurity scattering cross-section. Remarkably, different kinds of potential impurities (e.g. charged, neutral) can now be distinguished by qualitatively different energy dependence of scattering, yielding unique signatures in the resulting $\sigma(T)$. These signatures could be used to characterize notoriously unknown potential profile for high-quality 2D samples.

In particular, for the important example of *charged impurities* within a 2D layer, we show that the conductivity grows as $\sigma \propto \sqrt{T}$ as long as temperature is below a few Rydberg of the host material ($\text{Ry} = me^4/2\hbar^2$ where m is the effective carrier mass), crossing over to $\sigma \propto T$ for $T \gg \text{Ry}$ (Fig. 1). The latter linear T -dependence¹³ is

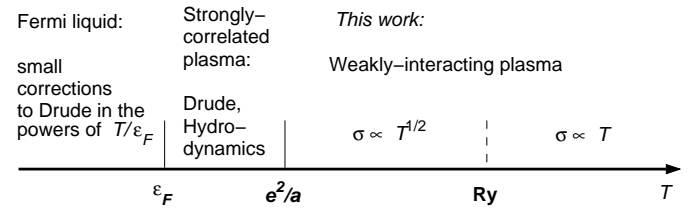


FIG. 1: 2D transport in the presence of charged disorder for $r_s = (e^2/a)/\epsilon_F > 1$. FL calculations^{1,2,3} provide small corrections to the Drude transport at $T \ll \epsilon_F$. For non-degenerate carriers, the perturbative result $\sigma \propto T^{13}$ is valid for $T \gg \text{Ry}, e^2/a$, while for $e^2/a \ll T \ll \text{Ry}$ we show that $\sigma \propto T^{1/2}$. For $\epsilon_F \lesssim T \lesssim e^2/a$ the system forms a strongly-correlated plasma where both Drude¹¹ and hydrodynamic¹² effects can be relevant. For $e^2/a < \epsilon_F$, i.e. $r_s < 1$, weakly-interacting Fermi gas crosses over to weakly-interacting classical plasma at $T \sim \epsilon_F$; the result $\sigma \propto T^{1/2}$ then holds for $\epsilon_F \ll T \ll \text{Ry}$.

thereby practically inobservable for two-dimensional electron gases (2DEGs) in GaAs heterostructures, since the phonon contribution dominates above $\Theta_D \approx \text{Ry} \approx 60 \text{ K}$. Hence, the single-particle explanation of Das Sarma and Hwang¹³ of the observed^{4,5,6,7} conductivity increase with temperature does not apply. For the other practical example, the strong *neutral impurities*, the conductivity is shown to decrease with temperature (as described below).

As a result, the superficial distinction between a “metal” ($d\sigma/dT < 0$) and an “insulator” ($d\sigma/dT > 0$) based simply on the *sign* of the derivative $d\sigma/dT$, does not hold – indeed, both behaviors are possible in a classical 2D metal (1). Of course, a true insulator is characterized by localized states as $T \rightarrow 0$, leading to activated conductivity dependence. Such a low- T analysis is beyond the scope of this work which considers only sufficiently high temperatures above the onset of localization.

In what follows, we first obtain the general result (6) for the T -dependent Drude conductivity in the regime (1) in terms of the energy-dependent impurity transport cross-section $\Lambda_{\text{tr}}(\epsilon)$, then we discuss the resulting $\sigma(T)$ for different kinds of potential disorder, and, finally, remark on the systems where one can practically observe the temperature-dependent Drude conductivity.

II. THE DRUDE TRANSPORT

The kinetic equation in the presence of an external in-plane field $\vec{\mathcal{E}}$

$$e\vec{\mathcal{E}}\mathbf{v}\partial_{\epsilon}f_0 = -\tau_{\epsilon}^{-1}\delta f, \quad \epsilon = mv^2/2 \quad (2)$$

is written in terms of the momentum relaxation rate

$$\tau_{\epsilon}^{-1} = n_i\Lambda_{\text{tr}}(\epsilon)v(\epsilon), \quad \Lambda_{\text{tr}} = \oint d\theta \frac{d\Lambda}{d\theta}(1 - \cos\theta). \quad (3)$$

Here $d\Lambda/d\theta$ is the differential scattering cross-section and n_i is the area density of impurities. The particular energy dependence of the scattering rate τ_{ϵ}^{-1} stems from that of the transport cross-section Λ_{tr} . The isotropic dc conductivity follows¹⁴:

$$\sigma = \frac{ne^2\bar{\tau}}{m}, \quad \bar{\tau} = \frac{\int d\epsilon \epsilon \tau_{\epsilon}(-\partial_{\epsilon}f_0)}{\int d\epsilon \epsilon(-\partial_{\epsilon}f_0)}, \quad (4)$$

where we assumed energy-independence of the 2D density of states in the case of the parabolic band. In the classical regime (1), quantum interference effects are irrelevant due to strong dephasing. As long as $T \gg e^2/a$, one can also neglect electron-electron interactions, such that the equilibrium velocity distribution is Maxwellian:

$$f_0(\epsilon(v)) = e^{(\mu-\epsilon)/T}, \quad e^{\mu/T} = \epsilon_F/T \ll 1. \quad (5)$$

Eqs. (4) and (5) yield

$$\sigma(T) = \sigma_0 \int_0^{\infty} \xi d\xi e^{-\xi} \frac{\lambda(\epsilon)}{\Lambda_{\text{tr}}(\epsilon)} \Big|_{\epsilon=\xi T}, \quad \sigma_0 \equiv \frac{e^2}{h} \frac{n}{n_i}, \quad (6)$$

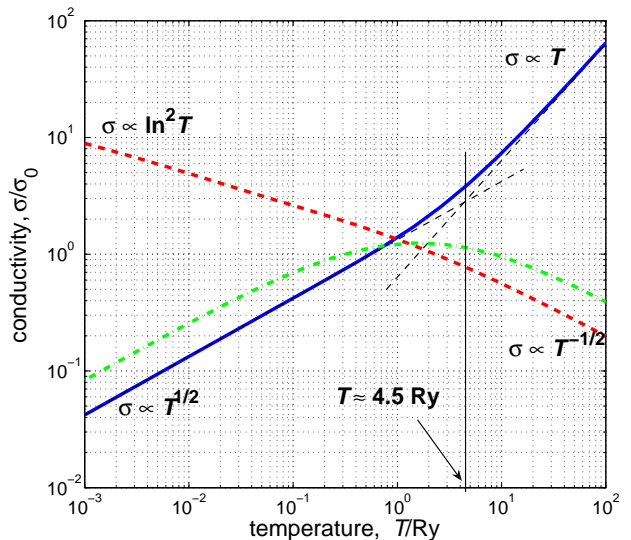


FIG. 2: Temperature-dependent Drude conductivity (6) in the units of $\sigma_0 = (e^2/h)n/n_i$. Solid blue line: charged impurities, Eq. (11), together with its asymptotic limits (thin dashed lines). Switching from $\sigma \propto T^{1/2}$ to $\sigma \propto T$ occurs at $T \approx 4.5 \text{ Ry}$. Dashed red line: neutral impurities (impermeable disks with radius $a = a_B$). Dash-dotted green line: 50% charged and 50% neutral impurities, with the same total n_i .

where energy-dependent wavelength $\lambda(\epsilon) = 2\pi/k(\epsilon)$, $\hbar k = mv(\epsilon)$. In other words, the temperature dependence of the Drude conductivity is determined by the energy dependence of the transport cross-section in the units of wavelength. For simple estimates, Eq. (6) gives

$$\sigma(T) \simeq \sigma_0 \frac{\lambda_T}{\Lambda_{\text{tr}}|_{\epsilon=T}}, \quad (7)$$

where $\lambda_T = 2\pi\hbar/\sqrt{2mT}$ is the temperature wavelength.

When multiple kinds of impurities are present, the scattering rates add up according to the Matthiessen rule. Thus the total transport cross-section entering Eq. (6)

$$\Lambda_{\text{tr}}(\epsilon) = c_1\Lambda_{\text{tr}}^{(1)}(\epsilon) + c_2\Lambda_{\text{tr}}^{(2)}(\epsilon) + \dots \quad (8)$$

where $c_j = n_i^{(j)}/n_i$ is the fraction of impurities of the sort j , and $n_i = \sum_j n_i^{(j)}$ is the total impurity concentration.

III. CHARGED IMPURITIES

For the e^2/r potential, the exact 2D differential cross section has been found in the seminal 1967 work of Stern and Howard¹⁵:

$$\frac{d\Lambda^c}{d\theta} = \frac{\alpha \tanh \pi\alpha}{2k \sin^2(\theta/2)}, \quad \alpha(v) \equiv \frac{e^2}{\hbar v}. \quad (9)$$

Here θ is the scattering angle, and the momentum transfer $q = 2\hbar k \sin \frac{\theta}{2}$. The result (9) has two distinct

limits. For small energies, $\epsilon \ll \text{Ry}$, the parameter $\pi\alpha \gg 1$, and the cross section is classical (indeed, it is \hbar -independent when $\tanh \pi\alpha \equiv 1$). Conversely, for high energies ($\epsilon \gg \text{Ry}$), the cross-section (9) with $\tanh \pi\alpha \approx \pi\alpha$ coincides with the Born approximation. Such a classical-to-quantum crossover is specific to 2D, whereas in 3D the Rutherford cross-section coincides both with the classical result and with the Born approximation.¹⁶

The corresponding 2D transport cross-section (3) reads

$$\Lambda_{\text{tr}}^c = (2\pi\alpha/k) \tanh \pi\alpha. \quad (10)$$

Notably, it is finite, with all scattering angles contributing roughly equally. This should be contrasted with the well-known logarithmically divergent transport cross-section for 3D Coulomb plasma¹⁷ (“Landau logarithm”), dominated by forward scattering processes.

The conductivity then follows from Eqs. (6) and (10):

$$\sigma^c(T) = \sigma_0 \int_0^\infty \frac{\xi d\xi e^{-\xi}}{\alpha \tanh \pi\alpha}, \quad \alpha^2 = \frac{\text{Ry}}{\xi T}. \quad (11)$$

The conductivity (11) grows with T (Fig. 2) since impurity scattering (9) weakens for faster moving carriers.

The asymptotic behavior of (11) is $\sigma^c \simeq \frac{3}{4}\sigma_0\sqrt{\pi T/\text{Ry}}$ at $T \ll \text{Ry}$, and $\sigma^c \simeq \frac{2}{\pi}\sigma_0 T/\text{Ry}$ at $T \gg \text{Ry}$. Practically, the switching between the two limits occurs when $T \approx 4.5 \text{ Ry}$ (Fig. 2, the two asymptotes cross). For $T \gtrsim 5 \text{ Ry}$ we agree with Ref. 13 where the Born approximation $\tau_\epsilon^{-1} \approx n_i \pi^2 e^4 / \hbar \epsilon$ was utilized in Eq. (3) [corresponding to the Fermi Golden Rule]. The limit $\sigma \propto \sqrt{T}$ is novel and relevant in the parameter range (1).

IV. NEUTRAL SCATTERERS

For any axially symmetric scatterer, the transport cross-section is given by¹⁵

$$\Lambda_{\text{tr}} = \frac{2}{k} \sum_{m=-\infty}^{\infty} \sin^2(\delta_{m+1} - \delta_m), \quad (12)$$

where δ_m is the scattering phase shift in the channel with orbital momentum m .

Consider an example of *strong neutral 2D scatterers* within the electron layer. Physically, they can originate from interface roughness or neutral atomic defects in a heterostructure. For sufficiently small ϵ_F and T , the carrier’s energy may become much smaller than the potential barrier which such a potential creates. It is then reasonable to model the scattering potential as being infinitely large within a disk of radius a , and zero outside. In this case, the scattering phase shifts $\tan \delta_m = J_m(ka)/Y_m(ka)$ are given in terms of the Bessel functions of the first and second kind, leading to

$$\Lambda_{\text{tr}}^n \simeq \begin{cases} 8a/3, & ka \gg 1; \\ \frac{\pi^2/k}{\pi^2/4 + \ln^2[2/(\gamma ka)]}, & ka \ll 1. \end{cases} \quad (13)$$

Here $\ln \gamma = 0.577\dots$ is Euler’s constant. Note the anomalously efficient scattering at wavelengths $\lambda = 2\pi/k \gg a$ exceeding the impurity size: $\Lambda_{\text{tr}}^n \sim \lambda/\ln^2(\lambda/a) \gg a$, i.e. the scattering cross-section is determined by the carrier wavelength rather than by the impurity size, thereby greatly exceeding the “geometric” limit. This is a known universal signature of low-energy 2D scattering.¹⁶

The estimate (7) yields

$$\sigma^n(T) \sim \sigma_0 \times \min \left\{ \ln^2 \frac{\epsilon_a}{T}, \left(\frac{\epsilon_a}{T} \right)^{\frac{1}{2}} \right\}, \quad \epsilon_a \sim \frac{\hbar^2}{ma^2}. \quad (14)$$

The exact conductivity $\sigma^n(T)$ for strong neutral scatterers calculated numerically using Eqs. (12) and (6), is shown in Fig. 2. Its asymptotic behavior for small and large T agrees with the qualitative estimate (14). In order to compare with the Coulomb scattering, we took the disk radius $a = a_B$ to be equal to the Bohr radius $a_B = \hbar^2/m\epsilon^2$, such that $\epsilon_a \sim \text{Ry}$; $a_B \sim 10 \text{ nm}$ for GaAs.

We also note that *weak short-range scatterers* yield temperature-independent conductivity. Indeed, the differential cross-section $d\Lambda/d\theta = |f(\theta)|^2$ in the Born approximation $f^{\text{Born}}(\theta) = -m\tilde{U}(q)/\hbar^2\sqrt{2\pi k}$ (Ref. 16) yields $\Lambda_{\text{tr}}^{\text{Born}} \propto \lambda$ for q -independent formfactor $\tilde{U}(q)$ corresponding to a short-ranged potential $U(r)$. Eq. (6) then results in $\sigma = 2\pi\sigma_0(\hbar^2/m\tilde{U})^2 = \text{const}$.

V. DISORDER SPECTROSCOPY

In realistic clean low-density samples multiple kinds of disorder, e.g. Coulomb impurities and neutral scatterers, are present. The conductivity (6) and (8) can then display a fairly complex sample-specific dependence on temperature, governed by relative contributions of different kinds of scatterers. Fig. 2 shows an example with $c^c = c^n = 0.5$.

Qualitatively different T -dependences (11) and (14) present a natural way to characterize disorder in clean 2D samples. For that one needs to operate at very low carrier densities $n \lesssim 10^9 \text{ cm}^{-2}$, when a temperature window (1) opens up. Fitting the conductivity (with the phonon contribution subtracted) to the result (6) and (8) will yield the disorder composition $\{n_i^{(j)}\}$. This way, the T -dependent transport can serve as the disorder spectroscopy. The connection with spectroscopy is not accidental: Formally, the conductivity is proportional to Laplace transform $\int_0^\infty d\epsilon e^{-\beta\epsilon}\varphi(\epsilon)$ of the quantity $\varphi(\epsilon) = \sqrt{\epsilon}/\Lambda_{\text{tr}}(\epsilon)$, where $\beta = 1/T$.

VI. CHARGED DISORDER IN GaAs HETEROSTRUCTURES

The result (11) based on the exact cross-section (9), predicts a novel $\sigma \propto \sqrt{T}$ conductivity dependence, characteristic of the classical limit of scattering (9).

The latter can be relevant for transport in clean dilute heterostructures.^{4,5,6,7,8,9,10} So far, the observed conductivity grows approximately linearly with temperature around $T \sim 1$ K.^{4,5,6,7} From the present analysis, the single-particle explanation¹³ for this observation based on the Born scattering cannot hold for GaAs, since, according to Fig. 2, the crossover to the Born regime would occur at $T \approx 300$ K which is practically inaccessible due to the dominant phonon scattering.^{18,19} The apparent discrepancy between the present single-particle theory yielding $\sigma \propto \sqrt{T}$, and the experiments^{4,5,6,7} strongly indicates the predominance of collective effects in transport. This is not surprising, since typical Coulomb energy $e^2/a \simeq 20$ K [corresponding to $n = 1 \times 10^{10} \text{ cm}^{-2}$], while the measurements were done for at least order-of-magnitude lower temperatures, in which case using the Maxwell distribution (5) in Eq. (4) is unjustified from the outset. For the lower densities, $n \lesssim 10^9 \text{ cm}^{-2}$, the present approach may apply, as long as the phonon contribution is controllably subtracted in the range (1).

Can the linear (RPA) screening affect the temperature dependence (11), and in particular, the crossover temperature $T \approx 5$ Ry? Below we argue that screening will only *weaken* the dependence $\sigma(T)$, and cannot lead to $\sigma(T) \propto T$ at low temperature.

Physically, screening changes the shape of the impurity potential in the following way: It fully preserves the strength of the e^2/r potential for distances $r \lesssim a_s$ shorter than the screening length, and cuts off the $1/r$ behavior for $r \gtrsim a_s$, where $a_s = \frac{T}{2\pi e^2 n} = \frac{a}{2} \frac{T}{e^2/a}$ [in the Fourier space, $2\pi e^2/k \rightarrow 2\pi e^2/(k + a_s^{-1})$]. The linear (RPA) screening is a mean-field effect, valid when the density fluctuations within the screening volume a_s^2 are small, fulfilled under the condition $na_s^2 \gg 1$ equivalent to $T \gg e^2/a$, compatible with the limit (1). This has the following consequences: (i) for $\epsilon_F < T < e^2/a$ relying on the RPA screening is unjustified. The single-particle transport calculation based on the Maxwell distribution (5) is also unjustified. Thus the approach¹³ of Das Sarma and Hwang does not apply to the experiments^{4,5,6,7} even if the authors were to use the correct scattering cross-section. (ii) For $T \gg e^2/a$, screening becomes asymptotically *irrelevant* for the Drude transport. Indeed, consider the region $r < a_s$ where the electron “feels” the unscreened impurity potential. Upon entering this region, its typical kinetic energy greatly exceeds the Coulomb field, $T \gg e^2/a_s$. Thus the scattering phase shifts yielding the cross-section (9) have parametrically large room to accumulate between $e^2/T \ll r \ll a_s$, leading to its nonperturbative limit. Moreover, the residual screening (truncation of the potential for $r \gtrsim a_s$) would further weaken the $\sigma(T)$ dependence, since, according to the above calculation [cf. Eqs. (6) and (14)], the conductivity

due to short-range disorder decreases with temperature. Thus the initial $\sigma \propto \sqrt{T}$ dependence would only weaken when the residual screening is taken into account.

As a result, the explanation¹³ suggested for the apparent linear growth of the conductivity with temperature,^{4,5,6,7} does not apply; the observed linear (and, generally, power-law⁸) T -dependence of the low-temperature conductivity remains an exciting unresolved problem.

VII. GRAPHENE WITH CHARGED DISORDER

The nonrelativistic scattering considered above can be applied to graphene samples where Dirac mass $m = \Delta/v_F^2$ can originate e.g. from symmetry-breaking between sublattices, such that gap $\Delta \sim 10 - 100$ meV.^{20,21} Half-filled band corresponds to chemical potential $\mu = -\Delta$ counted from the bottom of the “parabolic” band. The graphene electron system is nonrelativistic and non-degenerate as long as $T \ll \Delta$, since $\epsilon_F = Te^{-\Delta/T} \ll T$ [Eq. (5)]. When electron interactions (controlled by dielectric environment) are weak, $\alpha_g = e^2/\hbar v_F \ll 1$ where $v_F \simeq 10^6$ m/s, the effective Rydberg $\text{Ry}_g = \alpha_g^2 \Delta/2 \ll \Delta$. Hence, cf. Fig 1, the conductivity $\sigma \propto T^{1/2}$ for $T \ll \text{Ry}_g$ and $\sigma \propto T$ for $\text{Ry}_g \ll T \ll \Delta$. For strong interactions, $\alpha_g \sim 1$, $\text{Ry}_g \sim \Delta$ and the regime $\sigma \propto T$ never plays out. For $T \gg \Delta$ the system becomes relativistic, the cross-section scales as the wavelength,²² and the T -dependence of the Drude conductivity $\sigma \propto T^2$ comes solely from that of carrier density $n \propto T^2$, Ref. 23.

VIII. SUMMARY

To conclude, we considered temperature-dependent Drude transport in non-degenerate 2D electron systems. The Drude conductivity due to charged disorder behaves classically, $\sigma \propto T^{1/2}$ for temperatures below a few Rydberg, while neutral disorder results in decreasing $\sigma(T)$. These signatures can be utilized in determining disorder content of clean 2D samples in the limit (1). The decrease of the conductivity while reducing temperature does not necessarily signify a transition to an insulating state.

Acknowledgments

This work has benefited from discussions with M. Dykman and L. Glazman. Research was supported by NSF grants No. DMR-0749220 and No. DMR-0754613.

¹ B.L. Altshuler and A.G. Aronov, in *Electron-Electron Interactions in Disordered Systems*, edited by A.L. Efros and

M. Pollak (North-Holland, Amsterdam, 1985).

- ² G. Zala, B.N. Narozhny, and I.L. Aleiner, Phys. Rev. B **64**, 214204 (2001).
- ³ F. Stern and S. Das Sarma, Solid-State Electron. **28**, 211 (1985); A. Gold and V.T. Dolgoplov, Phys. Rev. B **33**, 1076 (1986); S. Das Sarma, Phys. Rev. B **33**, 5401 (1986).
- ⁴ Y. Hanein, U. Meirav, D. Shahar, C. C. Li, D. C. Tsui, and H. Shtrikman, Phys. Rev. Lett. **80**, 1288 (1998).
- ⁵ A. P. Mills, Jr., A. P. Ramirez, L. N. Pfeiffer, and K. W. West, Phys. Rev. Lett. **83**, 2805 (1999).
- ⁶ M. P. Lilly, J. L. Reno, J. A. Simmons, I. B. Spielman, J. P. Eisenstein, L. N. Pfeiffer, K. W. West, E. H. Hwang, and S. Das Sarma, Phys. Rev. Lett. **90**, 056806 (2003).
- ⁷ H. Noh, M. P. Lilly, D. C. Tsui, J. A. Simmons, L. N. Pfeiffer, and K. W. West, Phys. Rev. B **68**, R241308 (2003).
- ⁸ J. Huang, D. S. Novikov, D. C. Tsui, L. N. Pfeiffer, and K. W. West, Phys. Rev. B **74**, 201302(R) (2006); J. Huang, D. S. Novikov, D. C. Tsui, L. N. Pfeiffer, and K. W. West, cond-mat/0610320 (2006) (unpublished); J. Huang, D. S. Novikov, D. C. Tsui, L. N. Pfeiffer, and K. W. West, Int. J. Mod. Phys. B **21**, 1219 (2007); J. Huang, J. S. Xia, D. C. Tsui, L. N. Pfeiffer, and K. W. West, Phys. Rev. Lett. **98**, 226801 (2007).
- ⁹ M. J. Manfra, E. H. Hwang, S. Das Sarma, L. N. Pfeiffer, K. W. West, and A. M. Sergent, Phys. Rev. Lett. **99**, 236402 (2007).
- ¹⁰ L. H. Ho, W. R. Clarke, A. P. Micolich, R. Danneau, O. Klochan, M. Y. Simmons, A. R. Hamilton, M. Pepper, and D. A. Ritchie, Phys. Rev. B **77**, 201402(R) (2008).
- ¹¹ M.J. Lea and M.I. Dykman, Physica B **249**, 628 (1998) and references therein.
- ¹² B. Spivak and S. A. Kivelson, Annals of Physics **321**, 2071 (2006).
- ¹³ S. Das Sarma and E.H. Hwang, Phys. Rev. Lett. **83**, 164 (1999); Phys. Rev. B **68**, 195315 (2003).
- ¹⁴ T. Ando, A.B. Fowler, and F. Stern, Rev. Mod. Phys. **54**, 437 (1982).
- ¹⁵ F. Stern and W.E. Howard, Phys. Rev. **163**, 816 (1967).
- ¹⁶ L. D. Landau and E. M. Lifshits, *Quantum Mechanics (Non-Relativistic Theory)* (Elsevier, Oxford, 1977).
- ¹⁷ E.M. Lifshitz and L.P. Pitaevskii, *Physical Kinetics*, Pergamon, Oxford (1981).
- ¹⁸ B. K. Ridley, Rep. Prog. Phys. **54**, 169 (1991).
- ¹⁹ X.P.A. Gao, G.S. Boebinger, A.P. Mills, Jr., A.P. Ramirez, L.N. Pfeiffer, and K.W. West, Phys. Rev. Lett. **94**, 086402 (2005).
- ²⁰ G. Giovannetti, P.A. Khomyakov, G. Brocks, P.J. Kelly, J. van den Brink, Phys. Rev. B **76**, 073103 (2007).
- ²¹ S.Y. Zhou, G.-H. Gweon, A.V. Fedorov, P.N. First, W.A. de Heer, D.-H. Lee, F. Guinea, A.H. Castro Neto, and A. Lanzara, Nature Materials **6**, 770 (2007).
- ²² D. S. Novikov, Phys. Rev. B **76**, 245435 (2007).
- ²³ D. S. Novikov, Appl. Phys. Lett. **91**, 102102 (2007).